Wettability decay in an oil-contaminated waste-mineral mixture with dry-wet cycles

Sérgio D.N. Lourenço[1], School of Earth and Ocean Sciences, Cardiff University, Main Building, Park Place, Cardiff CF10 3AT, UK, lourenco@hku.hk , T: +852 39172672

Clare F. Wakefield, School of Earth and Ocean Sciences, Cardiff University, Main Building, Park Place, Cardiff CF10 3AT, UK

Christopher P. Morley, School of Chemistry, Cardiff University, Main Building, Park Place, Cardiff CF10 3AT, UK

Stefan H. Doerr, Institute of Environmental Sustainability, School of the Environment and Society, Swansea University, Singleton Park, Swansea SA2 8PP, UK

Robert Bryant, School of Engineering, Swansea University, Singleton Park, Swansea SA2 8PP, UK

Current address: Department of Civil Engineering, The University of Hong Kong, Haking Wong Building, Pokfulam Road, Hong Kong SAR

ABSTRACT

The dependency of soil particle wettability on soil water content implies that soils subjected to drying-wetting cycles become wettable with wetting and water repellent with drying. While this has been demonstrated widely, the results are contradictory when water repellent soils are subjected to a sequence of cycles. Added to this, past wettability measurements were seldom done in batches of samples collected from the field at natural or dry water contents, with little appreciation that slight particle size variations, different drying-wetting histories and fabric (as required by different wettability measurement methods) may alter the results. This note presents soil particle wettability – soil water content relations by means of an index test following staged drying and wetting paths over a period of 8 months for an untreated, oil contaminated anthropogenic soil (a mixture of slag, coal particles, fly ash and mineral particles) from Barry Docks (UK), a site formally used for oil storage, which is to be remediated and redeveloped for housing. The results revealed a decrease in the water repellency and increasing mineralization and bacterial activity with the wetting and drying cycles.

KEYWORDS: oil spills, soil particle wettability, dry-wet cycles

1. INTRODUCTION

Oil spills impregnate soil particles with water repellent organic coatings (Roy et al.,1998). Reclamation materials and soils contaminated by crude oil from Alberta's Oil Sands developed water repellency or reduced wettability (Hunter 2011; Quyum et al. 2002). The known dependency of soil particle wettability on soil water content implies that soils become wettable with wetting and water repellent with drying. While this is well known, the results are contradictory when water repellent soils are subjected to a sequence of drying-wetting cycles. Quyum et al. (2002) reported that soil particle wettability increased with the drying-wetting cycles in infiltration tests in oil contaminated soils, while Zhang et al. (2004) reported increased soil water repellency with the cycles in repacked degraded soil. In addition, little is known whether such relation is, like wettable soils, hysteretic (with the wetting path position below the drying path) and, how it relates to the critical water content at which wettability switches. These discrepancies are frequently explained by an interplay of microbiological activity (Jex et al. 1985), organic carbon dynamics (removal, transport and deposition) (Denef et al. 2001), and molecular re-arrangements (Graber et al. 2009).

Wettability measurements are frequently done in batches of samples collected from the field at a wide range of water contents (natural, air dried and oven dried), with little appreciation that variable particle size distributions, drying-wetting histories and fabric (sample preparation method) may influence the results (King 1981; Dekker and Ritsema 1994, 2000; de Jonge et al. 1999, 2007; Poulenard et al. 2004). There is therefore a need to conduct wettability measurements in the same samples as they dry or wet mimicking the Soil Water Retention Curve procedure for wettable unsaturated soils.

The aim of this study is to characterize the wettability behaviour (soil particle wettability versus soil water content) for an anthropogenic soil, an oil contaminated mixture of waste

(slag, coal particles and fly-ash) and mineral particles, collected from a former industrial site at Barry Docks, South Wales, United Kingdom subjected to continuous drying-wetting cycles.

2. STUDY SITE AND MATERIALS

The Barry Docks tank farm site (UK grid reference ST 11355 67047) is a highly heterogeneous fill of man-made materials, transported and *in-situ* soils. Barry Docks was until the 1970's a coal port. The current site was in part reclaimed from to the sea and extended by tipping locally sourced materials and furnace wastes. The land has had various industrial uses, the most recent being as an oil storage facility housing an extensive tank farm. The site is soon to be regenerated by the construction of residential dwellings. An engineered gravel cap has been installed across the site to prevent contact with the oil contaminants within the soil. With depth, the soil profile comprises made-ground of slag, coal particles, fly-ash, silica and limestone particles, which in turn are underlain by estuarine alluvium. A limestone (the St. Mary's Well Bay Formation) is the bedrock (Waters and Lawrence 1987). The oil contaminated material was collected from a number of locations around the footprint of the oil storage tanks using a hand auger and trowel (Fig. 1a). The oil-contaminated material was immediately below the engineered cover (around 10 cm depth) (Fig. 1b). From each location, around 1 kg of sample was collected and sealed in a plastic bag to preserve the *in-situ* water content.

The oil contaminated soils were characterised by the following: natural water content (oven drying at 105 °C), grain size distribution, mineralogy using X-ray powder diffraction (XRD) methods, specific gravity and loss on ignition test (at 400 °C for four hours) for total organic carbon content. For the specific gravity and loss on ignition tests, the measurements were

conducted for three samples and the results averaged. The loss on ignition was conducted after drying at 105°C. While there was a visible change in colour from dark to light brown, the results could have been affected by the previous drying at 105°C. Imaging to characterize the grain surface characteristics of representative samples were carried out using optical microscopy and environmental scanning electron microscopy (ESEM). Spot analysis using the energy dispersive X-ray analyser (SEM-EDX) was also undertaken to assist mineral identification.

The general properties of the soil samples are summarized in Table 1. Three samples from three different locations were tested in this study: B7, B11, B14. The soil-waste mixture was impregnated with oil, with no variations in its spatial distribution. The soils were predominantly granular, coarse sand-sized (size 0.1-2.0 mm) with clay content < 1% for B11 and B14, and an *in-situ* water content ranging between 16.4% and 23.0%. The specific gravity ranged between 2.48 and 2.05, the lower values probably due to the presence of fly ash and coal (Kim et al., 2005). The initial total organic carbon content ranged between 6.6% and 13.9%. These values include both the oil coatings and plant matter (fine roots). X-ray diffractograms for sample B7 identify a high silica content (attributed to quartz sand grains and silicate slag materials). Sample B11, was shown to be high in calcium carbonate (sourced from the nearby limestone cliff). B7 and B14, were also enriched by iron phases associated with the slag component. Some secondary mineralisation was observed from the SEM images. Clays were present in residual amounts (<1%) in samples B11 and B14. Exact mineral proportions could not be established since coal fragments, a component of the samples, cannot be detected by XRD (coal does not have a crystalline structure).

3. METHODS

The Water Drop Penetration Time was used to measure soil particle wettability during the wetting-drying cycles. The WDPT is an index test widely used amongst soil scientists (Letey et al. 2000), enabling wide comparison with values published in the literature and measurements in wetter and drier sandy samples. However, it may change the particle surface characteristics with the dissolution of organic carbon and decrease in surface tension (Zhang et al. 2004). Its infiltration times are also expected to decrease in drier samples due to a reduction in the unsaturated hydraulic conductivity, but should only present a problem for finer soils or lightly water repellent soils. The WDPT involves placing 3 de-ionized water droplets (each 80 μl) with a pipette on to the sample surface and recording the times for their complete infiltration. The average infiltration time of the three droplets is taken. Water repellent soils have longer infiltration times than wettable soils.

The sample preparation consisted of sieving to remove grains larger than 4 mm and consolidating in an oedometer (Bryant et al. 2007) at 50 kPa at constant water content conditions. Consolidation may have displaced the oil coatings and increased the packing of the soil-waste mixture due to the rearrangement of the grains. This differs from the field, where the material was loose and cohesionless. The sample was then removed from the oedometer proving-ring and placed in a Petri dish. Liquid paraffin wax was used to fill the annulus between the sample and the Petri dish wall to provide lateral support.

The procedure for the drying-wetting cycles followed that of a Soil Water Retention Curve whereby the same sample is dried or wetted in stages (described next) and pore water pressure/water content measurements conducted at equilibrium conditions (e.g. Lourenço et al. 2011). In this study, only the water content and soil wettability were measured. Equilibration means that the all parameters within the soil (e.g. water content and soil

wettability) are the same throughout the sample i.e. at the surface and inner parts. A period of equilibration is essential to ensure that water redistributes through the soil, after drying or wetting, before the water content and soil wettability are measured. The detailed procedure, in Fig. 2, consisted on the following stages:

1) Drying or wetting – the sample was dried in the atmosphere for a period ranging between 2-3 hours, at an ambient temperature of 20°C; wetting of the sample was from water vapour (to ensure homogeneous wetting) with the sample placed on a grid on a closed box above the water for a period <8 hours; water vapour was created by submerged mist generators (Mendes et al. 2008);
2) Equilibration – the Petri dish was closed for a period of 48 hours to ensure water redistribution within the soil; the 48 hours was assumed based on the small dimensions of the sample
3) Mass measurement – recording of the mass of the sample on a balance (0.01 g accuracy);
4) WDPT – placement of three water droplets on the sample's surface and recording with stop-watches the time for the three water droplets to infiltrate; to minimize drying from the sample's surface, the droplets were placed immediately after opening the Petri dish and closing afterwards; for the drying path, the placement of the droplets may have induced local wettability reversals (the area was locally wetted followed by the whole drying of the sample), this was unavoidable and represents a disadvantage of the WDPT.

The measurements started with the samples, untreated, at their natural water contents and steps 1) to 4) were repeated until the samples had air-dried. The process was then reversed, with the samples wetted until they regained their initial masses. The water contents varied between 25% (water clogged pores with no water penetrating) and 5% (a visibly dry

condition). All WDPT samples were subjected to 3 drying and wetting cycles. The total period of testing was 8 months.

4. RESULTS AND DISCUSSION

4.1. Soil particle wettability – water content relations

Gradual decay of wettability was observed with the cycles of drying and wetting (Table 3). Sample B7 was wettable from 20% to 17% water content, with the penetration times increasing to 38 minutes at 7% water content (Fig. 3). In the following cycles, the penetration time at the lowest water content (7%) decreased to 27 minutes in the wetting path 1, 14 minutes in the drying path 2 and 5 minutes in the wetting path 2. Sample B14 revealed a similar behaviour, with the penetration time at the lowest water content (14%) decreasing from 120 minutes, in drying path 1, to nearly 25 minutes in drying path 2 (Fig. 4). Sample B11 revealed a similar trend despite the results obtained for wetting path 1, which had led to it becoming more wettable (shorter penetration times) at the end of drying path 1 or the start of the wetting path 1 (Fig. 5). An interpretation for this wettability switch is provided in the next section.

The three samples remained fully wettable for increasing ranges of soil water content. Sample B7 remained wettable from 20% to 14% water content in drying path 1, increasing from 20% to 12% in drying path 2. Sample B14 revealed a similar trend, remaining wettable from 23% to 20 % water content in drying path 1, increasing the from 23% to 17% water content in the subsequent paths. Sample B11 behaved differently, remaining in a virtually wettable condition for the same water content range in the 3 paths: 23% to 15%.

In an air-dried state, soil particle wettability correlates with the total organic carbon content (Table 1). Sample B14, with the highest penetration times, had the highest initial total organic

carbon content (13.9%), followed by sample B7 with 10.7% total organic carbon content, and sample B11 with 6.6% total organic carbon content. This observed decrease in soil particle wettability with increasing total organic carbon content is in agreement with several studies (e.g. Dekker & Ritsema, 1994).

Note that the start of the wetting paths were frequently at lower water contents than the end of the drying curves (the case of the wetting path 1 in samples B11 and B14). This was possibly due to a lower Relative Humidity (RH) in the closed box at the initial stages of wetting. With time, the mist generators raised RH to near saturation water vapour inducing condensation onto the sample and increasing its water content.

4.2. Mineralization and microbiological activity

The samples developed a series of white spots across the surface with the sequence of drying-wetting cycles. The whitening of the samples was gradual and homogeneous across the exposed surface with time. Imaging of the white spots with an optical microscope and SEM-EDX revealed the following: (1) calcite precipitates (μm to mm sized) with a distinctive white colour that contrasted with the surrounding dark oil coatings (occurring as a continuous dark film) (sample B7 in Fig. 6a); (2) loose filaments crossing the pores and covering the particles and, micron sized open cylindrical structures attached to the surface of the grains (sample B11 in Fig. 6b and 6c). From their sizes, shapes and arrangements these structures were found to be biofilms, a mixture of microbial cells, extracellular polymeric material (sample B11 in Fig. 6d) produced by bacteria, and fungi. The bacteria are similar to *Actimomycetes* (typical soil bacteria) (Parkes & Sass 2012). An interpretation is that the initial oil coated calcite particles may have dissolved during wetting and precipitated during drying as new carbonates (without the oil coating). The bacteria may have also contributed to the formation of the new particles (biomineralization). Microorganisms contribute towards

the formation of minerals, in particular in limestone formations (Klappa 1979; Strong et al. 1992). In a comparable study, Feeney et al. (2006) found a similar decrease in the water repellency with dry-wet cycles and attributed the results to the leaching of hydrophobic compounds and molecular rearrangements. However, Jex et al. (1985) reported increased water repellency in samples that had developed biofilms after an incubation period at 100% Relative Humidity. The long-term duration of the cycles (8 months) may have also played a role, allowing sufficient time for the biofilm growth, together with the elevated temperature created by the mist generators during the wetting stages. The temperature (not measured) was estimated around 30°C. Note that the above observations apply to the surface exposed to the atmosphere. No observations were conducted on the internal parts of the sample.

The total organic carbon content was used to establish whether the observed whitening was due to the loss of the oil coatings during the drying-wetting cycles. After the dry-wet cycles, samples were collected from the bulk material of the samples (below the surface) and also the surface material (that had whitened) for loss on ignition tests. In comparison with the initial total organic carbon contents, the results showed a greater decrease in the total organic carbon at the surface than in the bulk material (Table 1). This could have been due to the physical washing of organic carbon from the surface (during the WDPT tests and when the sample achieved full saturation) and degradation of the organic carbon by the microbial activity. McKenna et al. (2002) showed that *Actimomycetes* ameliorate soil water repellency.

While no evidence was gathered linking the decrease in wettability with the biofilms, carbonates re-precipitation and decrease of carbon content, distinct mechanisms for the wettability decay are suggested. (1) The mineralization at the surface and formation of biofilms suggests that a new discontinuous surface made of clean minerals and microorganisms was created on top of the oily coatings. Consequently, the penetration times decreased since the new surface is not contaminated with water repellent substances. The

decrease in the total organic carbon content at the surface of the sample may have also contributed to the increased wettability. (2) Since no visible changes occurred to the surface of the samples, we speculate that the thresholds observed in the WDPT data in wetting path 1 of sample B11 arise from behaviour at the molecular level, and may be attributed to re-orientation of molecules at the air-oil interfaces (Cheng et al., 2009). In very general terms, some of the molecules that populate the air-oil interfaces are wettable at one end and water repellent at the other (Shaw, 1992). When these molecules are oriented with the water repellent end pointing away from the surface, such a configuration makes the oil coated grains water repellent. In the opposite configuration the wettable ends of the molecules are exposed to the atmosphere rendering the oil coated grains wettable (the configuration may thus be influenced by the changing nature of the surface to which the molecules adsorb). (3) Other factors may have contributed to the hysteresis in the drying and wetting paths: differences in the advancing and receding contact angles (Bachman et al. 2006); hydraulic hysteresis, as in wettable soils, due to the emptying and filling of ink-bottle pores (Wheeler et al. 2003); microstructural changes (Monroy et al. 2009). The tendency to wettable with drying-wetting cycles agrees with previous ESEM observations in wettable micron-sized silica spheres (Lourenço et al. 2012).

4.3. Geoenvironmental implications

The results highlight the dynamic nature of soil particle wettability and suggest that it is likely to gain in significance in the future if extreme dry events become more frequent. The results have applications within the built and natural environment: (1) In Brownfield sites with oil contamination, they highlight the importance of remediating the ground so that water repellency does not develop after dry weather spells, or in the case of dry climates, so that a permanent water repellent condition is avoided (Hunter, 2011). (2) The re-use of oil

contaminated soils *per se* or mixed with wettable materials (in fills for residential or transportation infrastructure, for instance) should be done with caution because it would generated wettable and water repellent areas which could lead to preferential flow through the wettable areas, and ultimately piping. Disposal of these materials may also generate similar issues. (3) The increased wettability following wetting and drying cycles due to the precipitation of carbonates and bacterial activity observed here suggests that this phenomenon can occur at other sites with limestone geology.

5. CONCLUSIONS

Soil particle wettability measurements in an oil-contaminated waste-mineral mixture revealed wettability decay with wetting and drying cycles. Mineralization of the surface with calcite, biofilm formation and decrease of carbon content were observed during the wetting and drying cycles, suggesting a link to the decrease in water repellency. Wettability switches were also observed after drying. Implications of these wettability changes are briefly discussed in the context of reusing or disposing these materials, in particular on their potential to develop preferential flow and piping. More research is required on the specific factors associated with the long-term changes in soil wettability, in particular for non-mineral granular materials.

ACKNOWLEDGEMENTS

This research was funded by the UK Engineering and Physical Sciences Research Council, grant EP/I008756/1 ‘The impact of water repellency on soil mechanics’. Laboratory support was provided by Sujung Ahn and Dr Emilia Urbanek (Swansea University) and Lindsey Axe, Peter Fisher and Anthony Oldroyd (Cardiff University). Access to the Barry Docks site was given by John Wilson (Persimmon Homes Ltd). Thanks are also due to Prof John Parkes and Dr Henrik Sass (Geomicrobiology Group, Cardiff University) and Prof Paul Wright (British Gas) for support with the microbiology.

REFERENCES

Bryant R, Doerr SH, Hunt G, Conan S (2007) Effects of compaction on soil surface water repellency. Soil Use and Management 23:238-24

Cheng S, Bryant R, Doerr SH, Wright CJ, Williams R (2009) Investigation of physico-chemical surface properties of soil particles and model materials with contrasting hydrophobicity using atomic force microscopy. Environmental Science and Technology 43 (17):6500–6506

De Jonge LW, Jacobsen OH, Moldrup P (1999) Soil water repellency: Effects of water content, temperature, and particle size. Soil Sci. Soc. Am. J. 63:437–442

De Jonge LW, Møldrup P, Jacobsen OH (2007) Soil-water content dependency of water repellency in soils: effect of crop type, soil management, and physical-chemical parameters. Soil Science 172 (8):577-588

Dekker LW, Ritsema CJ (1994) How water moves in a water repellent sandy soil: 1. Potential and actual water repellency. Water Resources Research 30 (9) 2507–2517

Denef K, Six J, Bossuyt H, Frey SD, Elliott E, Merckx R, Paustian K (2001) Influence of dry–wet cycles on the interrelationship between aggregate, particulate organic matter, and microbial community dynamics. Soil Biology and Biochemistry 33:1599–1611

Doerr SH, Shakesby RA, Dekker LW, Ritsema CJ (2006) Occurrence, prediction and hydrological effects of water repellency amongst major soil and land use types in a humid temperate climate. European Journal Soil Science 57:741-754

Feeney DS, Hallett PD, Rodger S, Bengough AG, White NA, Young LM (2006). Impact of fungal and bacterial biocides on microbial induced water repellency in arable soil. Geoderma 135:72-80

Graber ER, Tagger S, Wallach R (2009) Role of Divalent Fatty Acid Salts in Soil Water Repellency. Soil Sci. Soc. Am. J. 73:541-549

Hunter A (2011) Investigation of water repellency and critical water content in undisturbed and reclaimed soils from the Athabasca oil sands region of Alberta, Canada. MSc Dissertation, University of Saskatchewan

Jex GW, Bleakley BH, Hubbell DH, Munro LL (1985) High humidity-induced increase in water repellency in some sandy soils. Soil Sci. Soc. Am. J. 49:1177-1182

King PM (1981) Comparison of methods for measuring severity of water repellence of sandy soils and assessment of some factors that affect its measurement. Aust. J. Soil Res. 19:275–285

Kim B, Prezzi M, Salgado R (2005) Geotechnical Properties of Fly and Bottom Ash Mixtures for Use in Highway Embankments. Journal of Geotechnical and Geoenvironmental Engineering 131

Klappa CF (1979) Calcified filaments in Quaternary calcretes; organo-mineral interactions in the subaerial vadose environment. Journal of Sedimentary Research 49 (3) 955-968

Lourenço SDN, Gallipoli D, Augarde CE, Toll DG, Fisher PC, Congreve A (2012) Formation and evolution of water menisci in unsaturated granular media. Géotechnique 62 (3):193-199

Lourenço SDN, Gallipoli D, Toll D, Augarde C, Evans F (2011) A new procedure for the determination of the soil water retention curve by continuous drying using high suction tensiometers. Canadian Geotechnical Journal 48 (2):327-335

Letey J, Carillo MLK, Pang XP (2000) Approaches to characterize the degree of water repellency. J. Hydrol. 231–232:61– 65

McKenna F, El-Tarabily KA, Petrie S, Chen C, Dell B (2002) Application of actinomycetes to soil to ameliorate water repellency. Letters in Applied Microbiology 35:107–112

Mendes J et al. (2008) A system for field measurement of suction using high capacity tensiometers. In Toll D.G., Gallipoli D., Augarde C.E., Wheeler S.J. (eds). Unsaturated Soils: Advances in Geo-Engineering, CRC Press, 219-225

Monroy R, Zdravkovic L, Ridley A (2009) Evolution of microstructure in compacted London Clay during wetting and loading. Géotechnique 60 (2):105 –119

Parkes J., Sass H. (2012) Personal communication

Poulenard J, Michel JC, Bartoli F, Portal JM, Podwojewski P (2004) Water repellency of volcanic ash soils from Ecuadorian páramo: effect of water content and characteristics of hydrophobic organic matter. European Journal of Soil Science 55:487–496

Quyum A, Achari G, Goodman RH (2002) Effect of wetting and drying and dilution on moisture migration through oil contaminated hydrophobic soils. The Science of the Total Environment 296:77–87

Roy JL, McGill WB, Rawluk MD (1998) Petroleum residues as water-repellent substances in weathered nonwettable oil-contaminated soils. Can. J. Soil Sci. 79:367-380

Shaw DJ (1992) Introduction to Colloid and Surface Chemistry, 4th ed., Butterworth-Heinemann Ltd

Strong GE, Giles JRA, Wright VP (1992) A Holocene calcrete from North Yorkshire, England: implications for interpreting palaeoclimates using calcretes. Sedimentology 39:333–347

Waters RA, Lawrence DJD (1987) Geology of the South Wales Coalfield, Part III, the country around Cardiff, 3rd Edition, British Geological Survey

Wheeler SJ, Sharma RS, Buisson MSR, (2003) Coupling of hydraulic hysteresis and stress-strain behaviour in unsaturated soils. Géotechnique 53 (1):41-54

Zhang B, Peng XH, Zhao QG, Hallett PD (2004) Eluviation of dissolved organic carbon under wetting and drying and its influence onwater infiltration in degraded soils restored with vegetation. European Journal of Soil Science 55:725–737

LIST OF CAPTIONS

Table 1: Initial and final physical and chemical parameters for the WDPT tests; mineral proportions: high >50%, low <50%, residual <1%

Table 2: Wettability of the waste-mineral samples in an air dried condition (after first drying); the classification is from Doerr et al (2006)

Table 3: Wettability decay for samples B7, B11, B14 for each path at 10% water content (the lowest water content in common between samples B7 and B11)

Figure 1: Sample collection; (a) site location showing footprint of oil tanks (diameter = 6 m); (b) photograph showing the oil contaminated material underlying the engineering cap layer (bar = 10cm)

Figure 2: Testing sequence

Figure 3: Relations between the water drop penetration time and water content for 2 drying and wetting cycles (sample B7)

Figure 4: Relations between the water drop penetration time and water content for 1 drying and wetting cycle followed by 1 drying path (sample B14)

Figure 5: Relations between the water drop penetration time and water content for 1 drying and wetting cycle followed by 1 drying path (sample B11)

Figure 6: SEM images showing the formation of the new surface) General view of sample surface with white spots of calcite (sample B7), b) Details of fungal filaments formed on a particle surface (sample B11), c) Overview of fungal filaments formed on a particle surface (sample B11), d) continuous film of extracellular polymeric substances wrapping the grains (sample B11)

Table 1: Initial and final physical and chemical parameters for the WDPT tests; mineral proportions: high >50%, low <50%, residual <1%; exact mineral proportions could not be established since coal fragments, a component of the samples, cannot be detected by XRD

Sample	**Mineral proportions from X-ray powder diffraction**				**Total organic carbon content (%)**			***In-situ* water content (%)**	**Specific gravity**
	Quartz	Calcite	Magnetite & Maghemite	Illite	Initial (bulk material)	Final (bulk material)	Final (surface material)		
B7	High	Residual	Low	Not detected	10.7	9.7	6.2	19.8	2.40
B11	Low	High	Not detected	Residual	6.6	6.1	3.7	16.4	2.48
B14	Low	Low	Low	Residual	13.9	16.4	11.6	23.0	2.05

Table 2: Wettability of the waste-mineral samples in an air dried condition (after first drying); the classification is from Doerr et al (2006)

Sample	**Test**	**Measure unit**	**Classification**[a]
B7	WDPT	38 minutes	Severe
B11	WDPT	2.6 minutes	Moderate
B14	WDPT	120 minutes	Extreme

Table 3: Wettability decay for samples B7, B11, B14 for each path at 10% water content (the lowest water content in common between samples B7 and B11)

Sample	**WDPT (minutes)**			
	Drying path 1	**Wetting path 1**	**Drying path 2**	**Wetting path 2**
B7	9.0	0.7	2.3	0.8
B11	1.8	0.5	1.1	-
B14*	-	202.7	25.0	-

* At 14% water content

a


oil tanks footprint

b

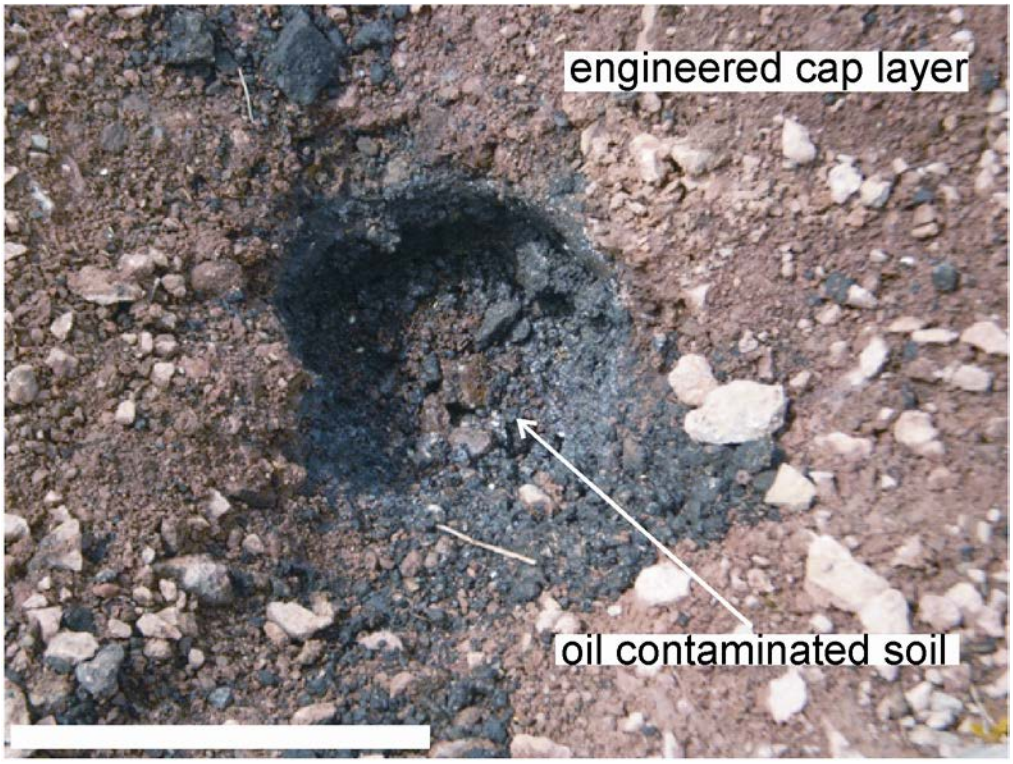
engineered cap layer
oil contaminated soil

Figure 1: Sample collection; (a) site location showing footprint of oil tanks (diameter = 6 m); (b) photograph showing the oil contaminated material underlying the engineering cap layer (bar = 10cm)

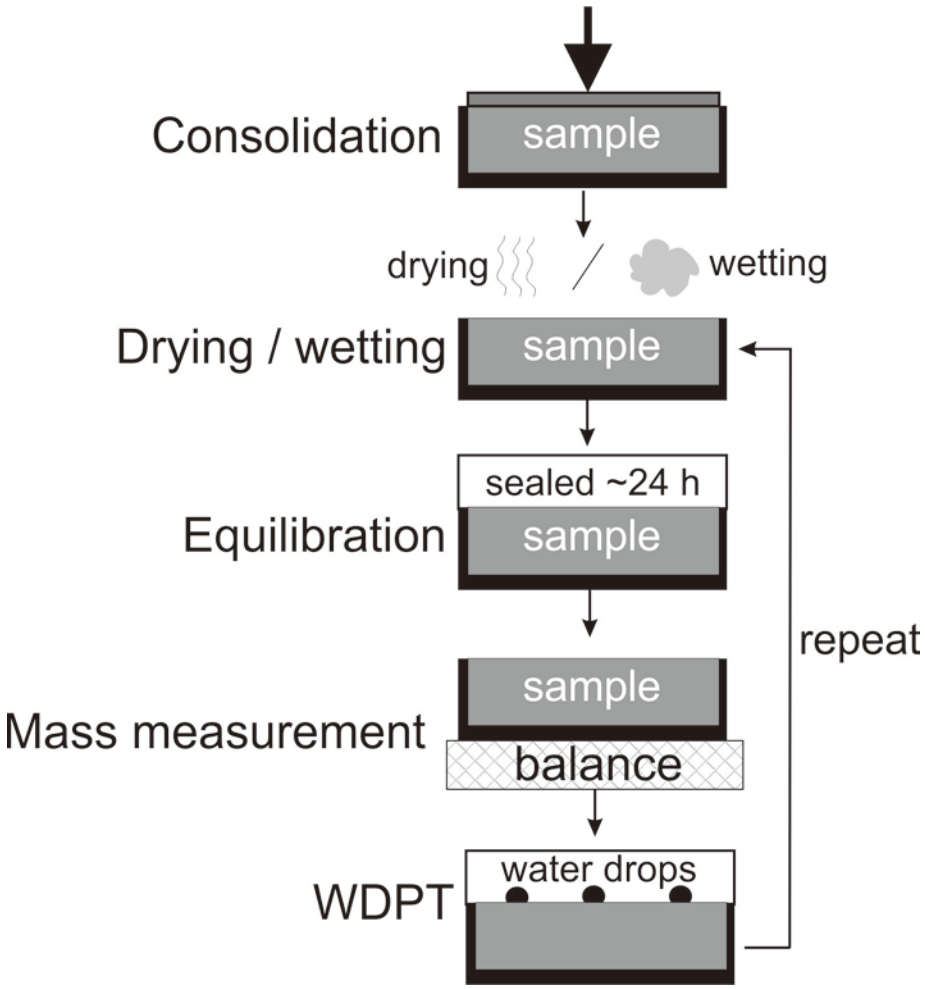

Figure 2: Testing sequence

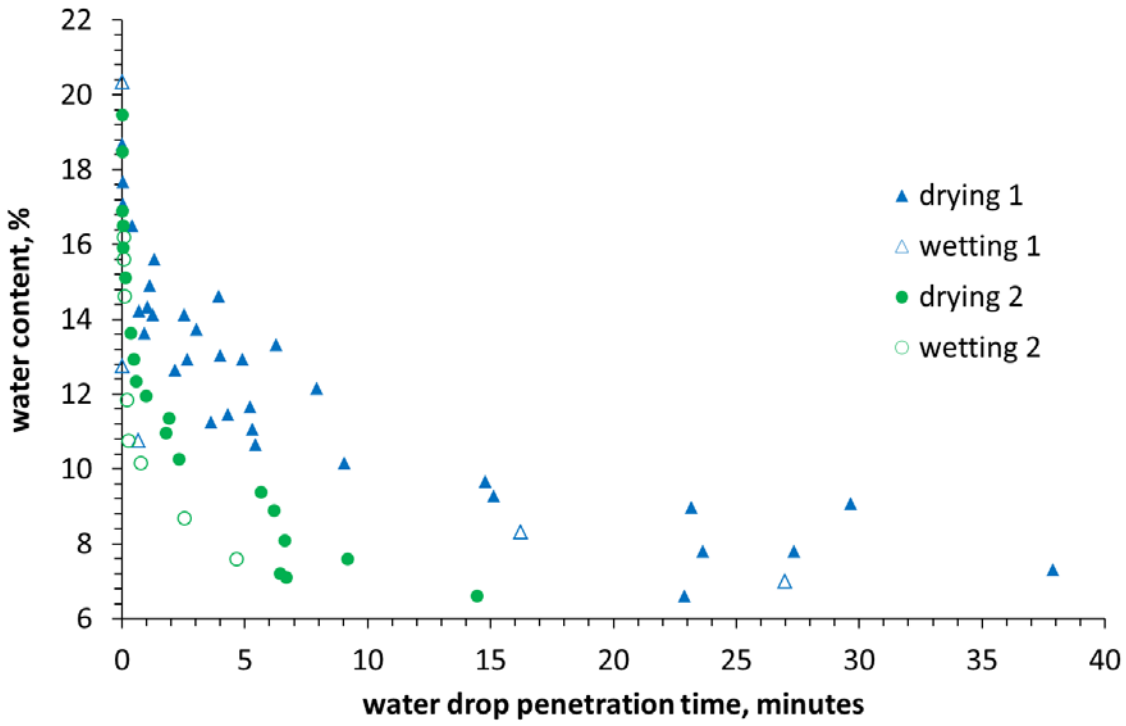

Figure 3: Relations between the water drop penetration time and water content for 2 drying and wetting cycles (sample B7)

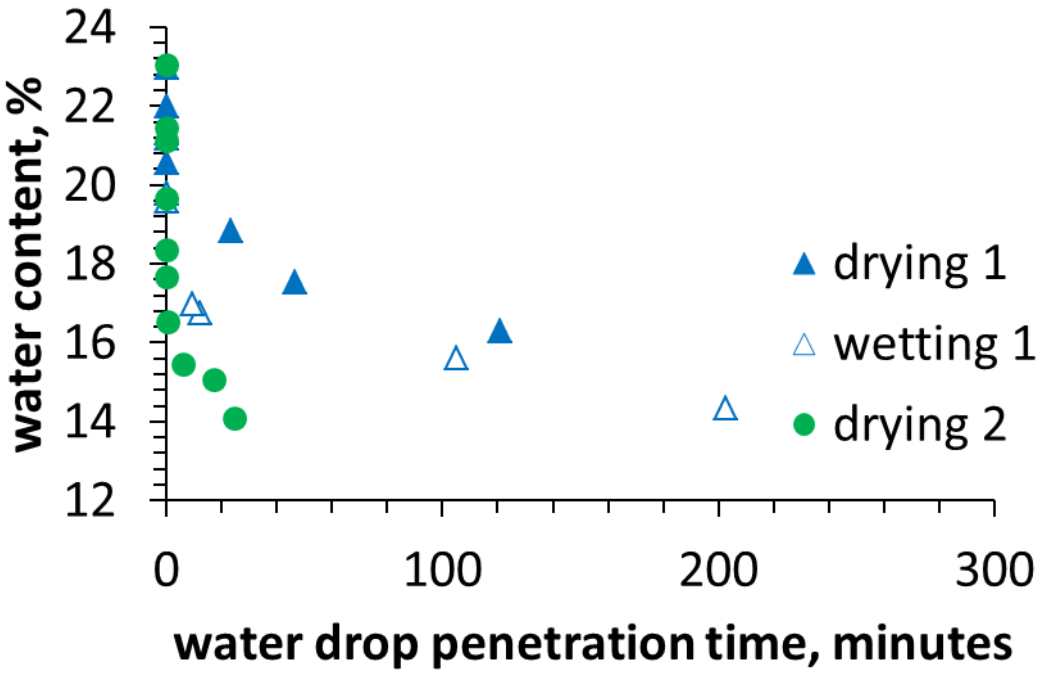

Figure 4: Relations between the water drop penetration time and water content for 1 drying and wetting cycle followed by 1 drying path (sample B14)

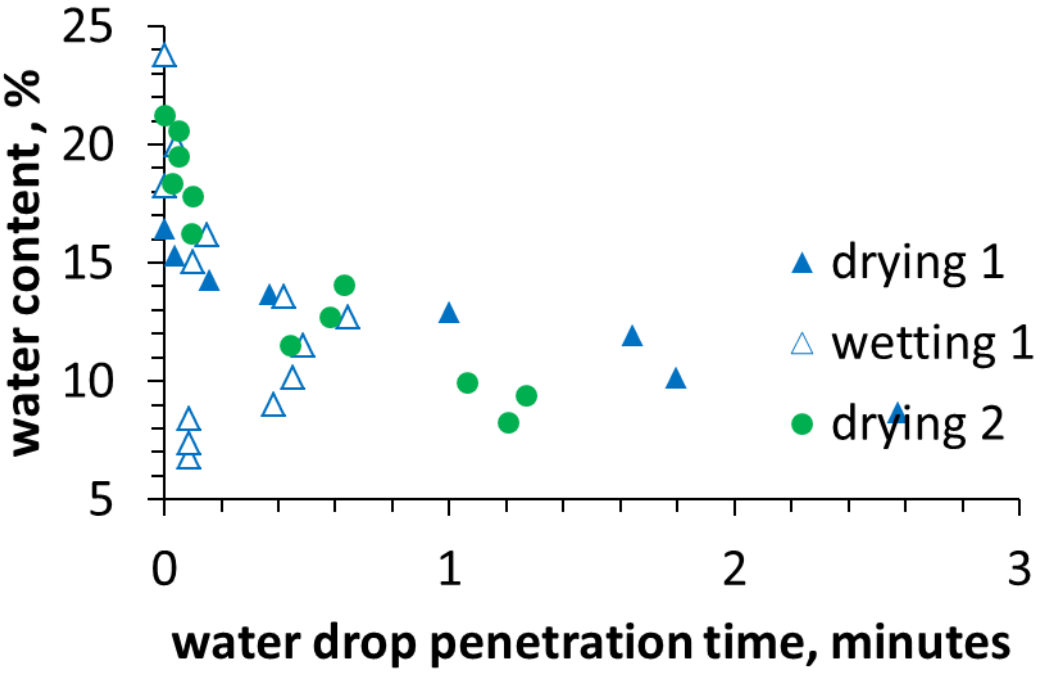

Figure 5: Relations between the water drop penetration time and water content for 1 drying and wetting cycle followed by 1 drying path (sample B11)

(a)

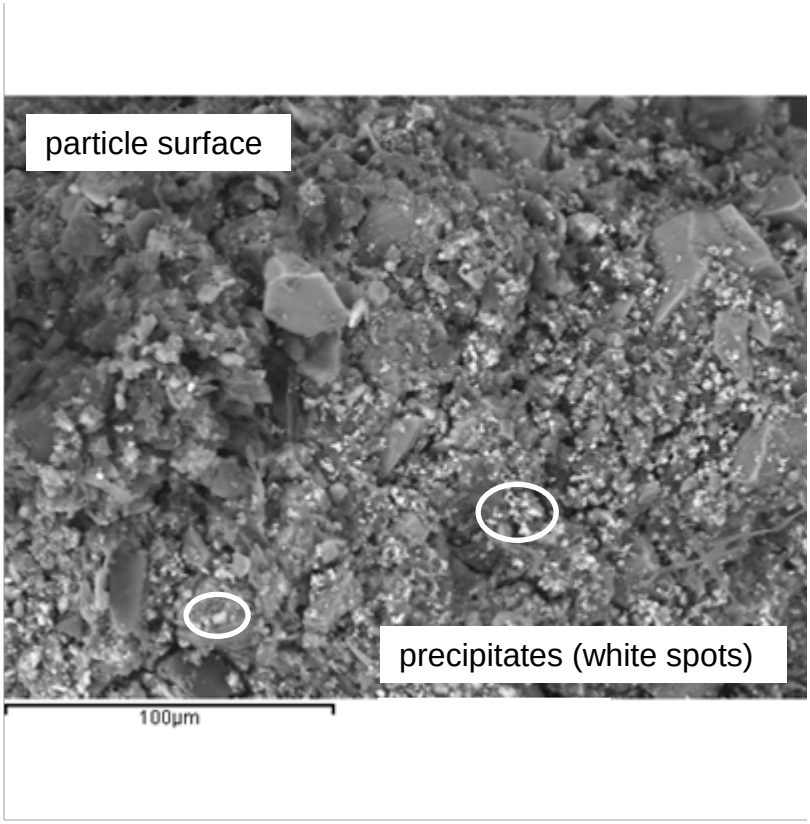
particle surface
precipitates (white spots)
100µm

(b)

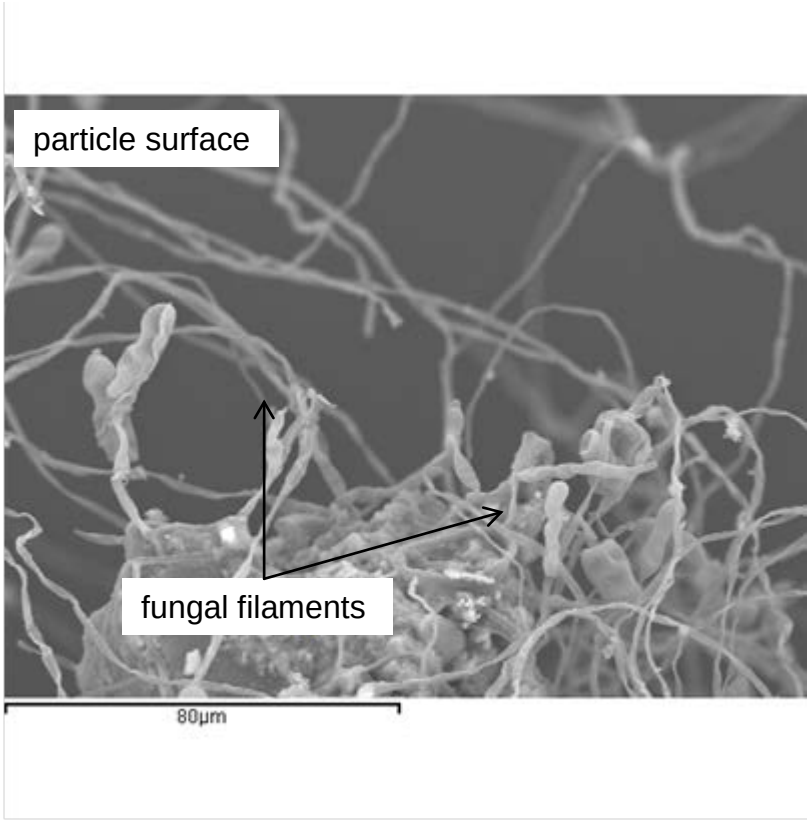
particle surface
fungal filaments
80µm

(c)

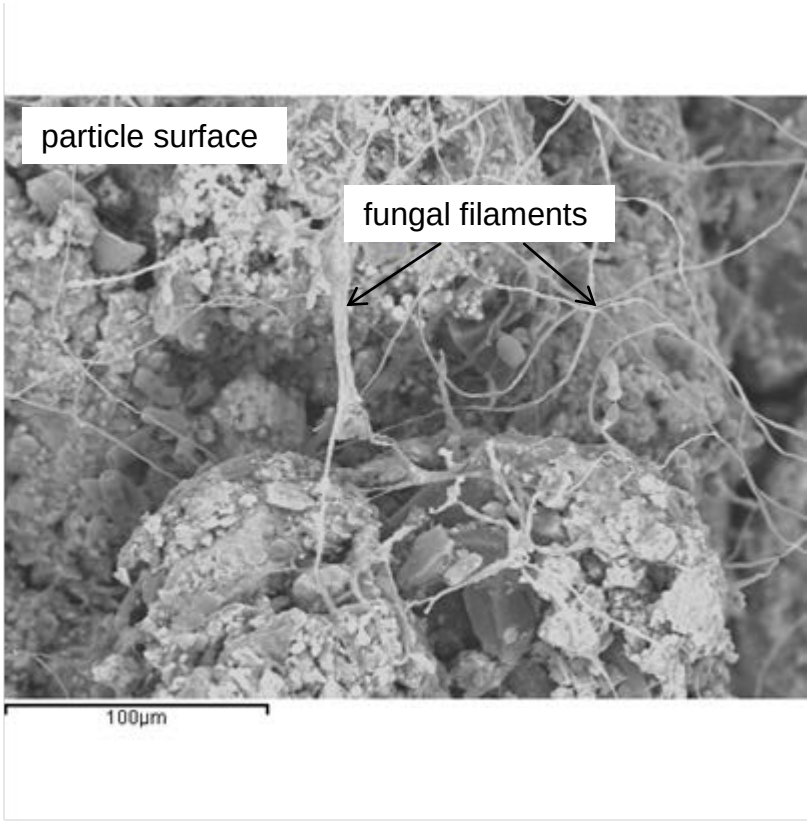
particle surface
fungal filaments
100µm

(d)

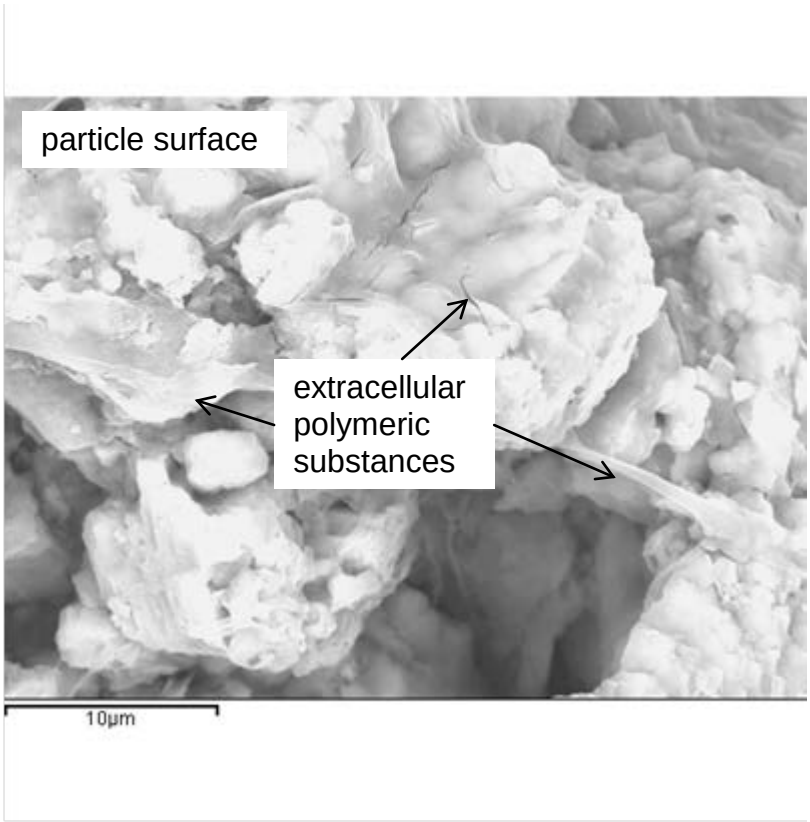
particle surface
extracellular
polymeric
substances
10µm

Figure 6: SEM images showing the formation of the new surface) General view of sample surface with white spots of calcite (sample B7), b) Details of fungal filaments formed on a particle surface (sample B11), c) Overview of fungal filaments formed on a particle surface (sample B11), d) continuous film of extracellular polymeric substances wrapping the grains (sample B11)